



Hydrated electron (e_{aq}^-) generation from phenol/UV: Efficiency, influencing factors, and mechanism

Jia Gu^a, Jun Ma^{a,*}, Jin Jiang^a, Ling Yang^{b,*}, Jingxin Yang^c, Jianqiao Zhang^a, Huizhong Chi^a, Yang Song^a, Shaofang Sun^a, Wei Quan Tian^d

^a State Key Laboratory of Urban Water Resource and Environment, School of Municipal and Environmental Engineering, Harbin Institute of Technology, Harbin, Heilongjiang 150090, PR China

^b MIIT Key Laboratory of Critical Materials Technology for New Energy Conversion and Storage, School of Chemistry and Chemical Engineering, Harbin, Heilongjiang 150080 PR China

^c Shenzhen Key Laboratory of Water Resource Application and Environmental Pollution Control, Harbin Institute of Technology Shenzhen Graduate School, Shenzhen, Guangdong 518055, PR China

^d College of Chemistry and Chemical Engineering, Chongqing University, Chongqing 401331, PR China



ARTICLE INFO

Article history:

Received 16 May 2016

Received in revised form 5 July 2016

Accepted 19 July 2016

Available online 19 July 2016

Keywords:

Phenol

UV irradiation

Hydrated electron

Phenoxy radical

Quantum chemical calculations

ABSTRACT

A phenol/UV (253.7 nm) process to generate hydrated electron (e_{aq}^-) was experimentally and theoretically studied in the present work, where monochloroacetic acid (MCAA) was selected as the probe of e_{aq}^- . It was demonstrated that the e_{aq}^- generation efficiency was dependent on the phenol concentration and pH. To interpret the dependence, a mechanism for the generation of e_{aq}^- from phenol was proposed and confirmed by the quantum chemical calculations. Theoretically, phenol could eject e_{aq}^- and phenoxy radical ($C_6H_5O^\bullet$), followed by the addition of hydroxyl ion (OH^-) to $C_6H_5O^\bullet$, and the simultaneous formation of phenol and *p*-hydroquinone was accomplished by hydrogen abstraction of the adduct with $C_6H_5O^\bullet$ as hydrogen acceptor (period I). The generated *p*-hydroquinone could also release e_{aq}^- with *p*-benzoquinone as the product (period II). Totally, one mole of phenol could generate four moles of e_{aq}^- via two periods, and two moles were generated in period I and two moles were in period II. Experimentally, e_{aq}^- could be ejected from phenol and phenolate, and the molar ratios of the species were determined by pH. Kinetically, the energy barriers of the electron release from phenol and phenolate were 63.7 kcal mol⁻¹ and 62.3 kcal mol⁻¹, respectively, which confirmed that the generation of e_{aq}^- from phenolate was much more efficient than that from phenol. These results may promote the development of novel e_{aq}^- reduction processes based on the phenolic compounds, since they are abundant in the environment.

© 2016 Elsevier B.V. All rights reserved.

1. Introduction

With the standard reduction potential of about -2.9 V [1], hydrated electron (e_{aq}^-) is one of the most reductive species [1], and the structure of e_{aq}^- can be simplified as a known number of oriented water molecules with an excess electron centered [2]. e_{aq}^- can react with many species through a one-electron transfer process [1], in which the existence and the availability of vacant orbital in the species are dominant, and the rate constants are from $10^1\text{ L mol}^{-1}\text{ s}^{-1}$ up to the diffusion controlled limit [1].

Recently, e_{aq}^- based advanced reduction processes (ARPs) [3] have drawn attention for the remediation of contaminated environ-

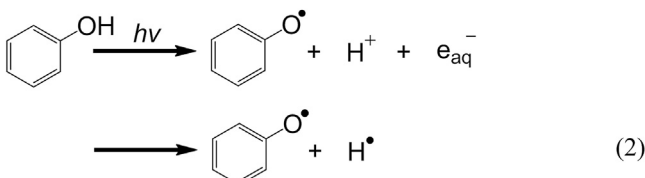
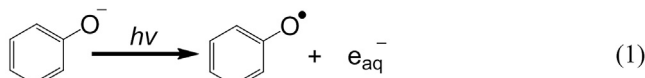
ments, especially for the reductive dehalogenation of halogenated organic compounds (HOCs) by the UV photolysis of some common inorganic reducing agents (e.g., sulfite, iodide, ferrous iron, etc) [4–9]. For instance, Li et al. have reported that monochloroacetic acid (MCAA) can be dechlorinated by sulfite/UV process [4]. In the process, the UV photolysis of sulfite can produce e_{aq}^- and SO_3^{2-} , and e_{aq}^- is the dominant reactive species accounting for the dechlorination [4]. Qu et al. found that the decomposition of perfluorooctanoic acid could be induced by e_{aq}^- generated in the UV–KI system, in which I^\bullet , I_2 , I_3^- , and I_2^- were the intermediates [5]. Calza et al. observed that light-excitation could lead the generation of e_{aq}^- from the ferrocyanide ion, and the generated e_{aq}^- was responsible for the reductive degradation of chloromethanes [6]. However, there have been few studies about the reductive degradation of pollutants by e_{aq}^- ejected from the phenolic compounds

* Corresponding authors.

E-mail addresses: majun@hit.edu.cn (J. Ma), yangling@hit.edu.cn (L. Yang).

[10,11], which are common organic electron donors [12] and widely distributed in the environment [13].

Several studies have reported that e_{aq}^- can be generated by the photolysis of phenol (the model of phenolic compounds) at 253.7 nm [14–16], as shown in the reactions (1) and (2). While, the detailed mechanism of the transformation of phenol is still a matter of debate. Joschek et al. have studied the photooxidation of phenol without oxygen in the solution under the steady irradiation at 253.7 nm, and they found that phenol could be transformed to *p*-benzoquinone [14], and the intermediate – *p*-hydroquinone was formed by cleavage reaction of the dimerization product [carbon–oxygen dimerization of phenoxyl radical ($C_6H_5O^\bullet$)] [14,17]. Distinctively, Tomkiewicz et al. found that *p*-hydroquinone was generated from an adduct (the addition of OH^- to $C_6H_5O^\bullet$) with hydrogen abstraction by another $C_6H_5O^\bullet$ [18]. In addition, Bussandri et al. found that the e_{aq}^- generation by the photolysis of phenol at 193 nm and 266 nm was accelerated with the increase of solution pH from acidic to basic [19], while, the reason for the dependence upon pH should be confirmed. Moreover, little is known about the stoichiometric ratio of phenol to the generated e_{aq}^- during the UV photolysis of phenol.



In the present work, recalcitrant monochloroacetic acid (MCAA) [20] was used as the probe of e_{aq}^- ($1.0 \times 10^9 \text{ M}^{-1} \text{ s}^{-1}$) [1], and the generation of e_{aq}^- in the phenol/UV process was studied by the degradation of MCAA. Firstly, the e_{aq}^- generation efficiency in the process was confirmed. Then, the influence of variables (e.g., the phenol concentration, the MCAA concentration, and pH) on the generation of e_{aq}^- was explored. Further, the mechanism of the e_{aq}^- generation from phenol was proposed and supported by the quantum chemical calculations, and the stoichiometric ratio of phenol to the generated e_{aq}^- was experimentally and theoretically determined. Finally, the generation rate of e_{aq}^- was determined to calculate the quantum yield of e_{aq}^- in the process, which could help to characterize the phenol/UV process.

2. Experimental

2.1. Materials and reagents

All chemicals were dissolved in deoxygenated ultra-pure water ($18.2 \text{ M}\Omega \text{ cm}$) as obtained commercial products without further purification, and the ultra-pure water was produced from a Milli-Q biocel system. Phenol (ACS reagent, $\geq 99.0\%$), (+)-catechin (analytical standard, $\geq 99.0\%$), thymol (analytical standard, $\geq 99.9\%$), *p*-cresol (analytical standard, 99.0%), *p*-benzoquinone (reagent grade, $\geq 98\%$), sodium monochloroacetate (98%), acetic acid (ACS reagent, $\geq 99.7\%$), potassium hydroxide (ACS reagent, $\geq 85\%$), sodium chloride (ACS reagent, $\geq 99.0\%$), sodium hydroxide (ACS reagent, $\geq 97.0\%$), sodium tetraborate decahydrate (ACS reagent, $\geq 99.5\%$), sodium phosphate dibasic (ACS reagent, $\geq 99.0\%$), sodium phosphate monobasic monohydrate (ACS reagent, 98.0–102.0%), hydrochloric acid (ACS reagent, 37%), dichloromethane (ACS reagent, $\geq 99.5\%$), sodium sulfate (ACS reagent, $\geq 99.0\%$), potassium

iodide (ACS reagent, $\geq 99.0\%$) and potassium iodate (ACS reagent, 99.5%) were supplied by Sigma-Aldrich. Methanol (HPLC Grade) was from Fisher Chemical. Hydrogen peroxide (H_2O_2 , 35% v/v, stab.) was purchased from Alfa Aesar. Nitrogen gas (N_2) was of high purity ($\geq 99.99\%$).

2.2. Experimental procedure

A 1000 mL sealed cylindrical borosilicate glass reactor was used to conduct the photolysis experiments with a 15 W low-pressure mercury UV lamp (253.7 nm, ozone-free, GPH303T5L, Light Sources) as the UV source, and the reactor was similar to that used by Li et al. [4]. By the methods described in a previous research [4], the photon flux (I_0) from the UV source to the solution, the average fluence rate (I_s) and the effective path length (L) were determined to be $(4.15 \pm 0.02) \times 10^{-6}$ einstein s^{-1} , 1.47×10^{-8} einstein $\text{s}^{-1} \text{ cm}^{-2}$ (6.94 mW cm^{-2}) and $(3.54 \pm 0.01) \text{ cm}$, respectively.

The temperature was controlled at $(25 \pm 0.5)^\circ\text{C}$. The pH from 6.2–12.3 was adjusted by phosphate buffer (10 mM), borate buffer (10 mM) and sodium hydroxide (10 mM), and the buffers showed negligible absorption at 253.7 nm. Nitrogen gas (N_2 , $\geq 99.99\%$) was used to remove dissolved oxygen from the solutions to guarantee the deoxygenated conditions. The addition of phenol was 0.2 mM in the solutions unless otherwise noted. The samples were periodically withdrawn and analyzed without capture of residual phenol for the negligible consumption of MCAA by phenol. All experiments were repeated at least in triplicate independently, and the results are presented by average values and standard deviation ($\pm SD$).

For identification of the reaction products by GC/MS–MS analysis, the reaction between 0.25 mM MCAA and 0.2 mM phenol was carried out at pH 12.0 and 25°C for 20 min in deoxygenated solution. The samples of the reaction were extracted into acidic ($\text{pH} = 2.0$), neutral ($\text{pH} = 7.0$) and basic ($\text{pH} = 12.0$) phases with dichloromethane (CH_2Cl_2), and the extract was then dried by anhydrous sodium sulfate, followed by filtration with a membrane in syringe filters of $0.45 \mu\text{m}$ pore size, and the pH of samples was adjusted to 7.0 and 2.0 by HCl.

2.3. Analytical methods

A pH meter (UB-7, Denver Instrument) was used to measure the solution pH. UV–vis absorbance spectra of phenol and phenolate was determined by a Varian Cary 300 UV–vis spectrometer from USA. The qualitative and quantitative analysis of chloride anion and monochloroacetate anion was accomplished by an ion chromatograph (Dionex ICS-3000), and 30 mM KOH was used as isocratic eluent at a flow rate of 1.0 mL min^{-1} , and the suppressor current was set to 75 mA. Phenol was determined by a Waters 1525 high performance liquid chromatography (HPLC), which was equipped with a Waters 2487 dual λ absorbance detector, and a Waters symmetry C18 column ($150 \text{ mm} \times 4.6 \text{ mm}$, $5 \mu\text{m}$) was used for chromatographic separation. Phenol was quantified at $\lambda = 270 \text{ nm}$, with an eluent of 0.1% acetic acid and methanol [60:40 (v/v)] at a flow rate of 1.0 mL min^{-1} . Reaction products were identified by GC/MS–MS (Agilent 7890 B MSD 7000C), and a HP-5 column ($30 \text{ m} \times 0.32 \text{ mm}$ internal diameter $\times 0.25 \mu\text{m}$) was employed for the separation. The GC/MS–MS analysis was performed in a temperature programmed mode: an initial temperature of 40°C was held for 10 min, and the temperature climbed up to 100°C at $12^\circ\text{C min}^{-1}$, then to 200°C at 5°C min^{-1} , finally to 270°C at $20^\circ\text{C min}^{-1}$, and this was followed by an isothermal stage which lasted 5 for minutes [21]. The split ratio was 10:1, and the column flow rate was 1.1 mL min^{-1} . The MS parameters of interface temperature, ionization mode and electron energy were set to 300°C , El^+ , 70 eV, respectively.

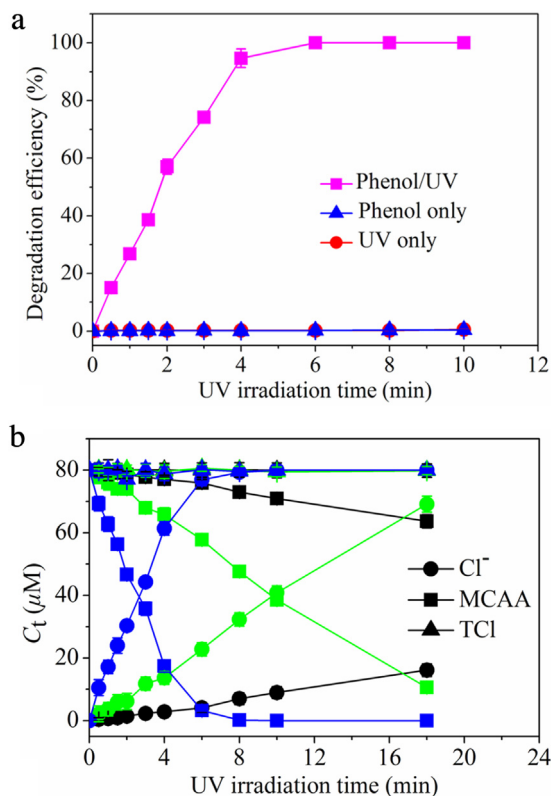


Fig. 1. (a) Degradation efficiency of MCAA (50 μM) in the phenol/UV process at pH 12.0. (b) Total mass balances of chlorine (TCI) during the degradation of MCAA (80 μM) in the phenol/UV process at different pH [6.2 (black), 9.2 (green), 12.0 (blue)]. Total chlorine (TCI) was calculated by $\text{TCI} = [\text{MCAA}] + [\text{Cl}^-]$. (For interpretation of the references to colour in this figure legend, the reader is referred to the web version of this article.)

2.4. Computation details

In order to verify the mechanism of e_{aq}^- generation from phenol, the density functional theory (DFT) based calculations were performed to support the homogeneous gas-phase transformation of phenol without environmental effect. More details are shown in the Supporting information (Text S1).

3. Results and discussion

3.1. The generation of e_{aq}^- in the phenol/UV process

As an e_{aq}^- probe [1], the addition of MCAA was used to verify the generation of e_{aq}^- in the phenol/UV process. Because the dissolved oxygen can efficiently quench e_{aq}^- ($1.9 \times 10^{10} \text{ M}^{-1} \text{ s}^{-1}$) [1], the reaction solutions were deaerated by purging with N_2 gas to minimize the interference. Phenol has two dominant forms – $\text{C}_6\text{H}_5\text{O}^-$ and $\text{C}_6\text{H}_5\text{OH}$ with $\text{p}K_{\text{a}} = 9.98$ [22] (Fig. S3a), and $\text{C}_6\text{H}_5\text{O}^-$ shows the stronger UV absorption at 253.7 nm (Fig. S3b). Fig. 1a demonstrates the degradation efficiency of MCAA in the phenol/UV process at pH 12.0, where $\text{C}_6\text{H}_5\text{O}^-$ is the dominant form. The direct photolysis of MCAA was negligible (less than 1% of 50 μM within 10 min) for its weak UV absorption at 253.7 nm [20]. The complete degradation of 50 μM MCAA in the presence of 0.2 mM phenol was achieved in 6 min under the UV irradiation (I_0/V) of 4.15×10^{-6} einstein $\text{L}^{-1} \text{ s}^{-1}$ at pH 12.0, and the pseudo-zero-order rate constant (k) of MCAA was $(11.84 \pm 1.40) \mu\text{M min}^{-1}$. In the control experiment, the direct degradation of MCAA by phenol (0.2 mM) was less than 2% within 24 h at pH 12.0 without UV irradiation, even though MCAA can react with the phenolic compounds [23]. So, it could be concluded that

Table 1

Rate Constants (k) of MCAA (80 μM) Degradation and Chloride Ion Formation in the Phenol/UV Process.

pH	Species	k ($\mu\text{M min}^{-1}$)	R^2
6.2	MCAA	0.9149 ± 0.0251	0.9925
	Cl^-	0.9065 ± 0.0245	0.9928
9.2	MCAA	3.9300 ± 0.0739	0.9965
	Cl^-	3.9154 ± 0.0679	0.9970
12.0	MCAA	15.0072 ± 0.5077	0.9932
	Cl^-	14.7316 ± 0.3990	0.9956

some reactive species were produced for the MCAA degradation in the process.

The photolysis of phenol can produce some reactive species [reactions (1) and (2)], e.g., e_{aq}^- , H^\bullet , and $\text{C}_6\text{H}_5\text{O}^\bullet$, as reported in some previous studies [14–16]. To verify their roles, the mass balances of chlorine during the kinetic runs were evaluated at different pH, as shown in Fig. 1b and Table 1. As can be seen in Fig. 1b, the degradation of MCAA and the formation of Cl^- was simultaneous. Quantitatively, the rates in Table 1 revealed that the chlorine in MCAA was released as Cl^- (more than 98%) through a reductive process. H^\bullet (the standard reduction potential of about -2.3 V) [1] and e_{aq}^- (-2.9 V) [1] are more reductive than $\text{C}_6\text{H}_5\text{O}^\bullet$ (about 0.8 V) [24], which obviously indicates that e_{aq}^- and/or H^\bullet accounted for the degradation of MCAA. However, as reported in a previous research, H^\bullet reacts with MCAA by abstracting H without Cl^- release [1]. Therefore, e_{aq}^- was the primary reactive species responsible for the degradation of MCAA even at pH 6.2. The dechlorination of MCAA at different pH confirmed the generation of e_{aq}^- in the phenol/UV process indirectly.

3.2. Influence of variables on the generation of e_{aq}^- in the phenol/UV process

3.2.1. Phenol

For the initiation [14] and photosensitization [14] in the process, the influence of phenol concentration on the generation of e_{aq}^- in the process was studied at pH 12.0. Fig. 2a shows that the degradation efficiency of MCAA was dependent on the phenol concentration when the concentration was below 0.3 mM, and then it was almost invariable. Fig. 2b presents a positive linear correlation between k and the phenol concentration (below 0.3 mM), with $k/[\text{phenol}]_0 = (62.12 \pm 3.73) \text{ min}^{-1}$. The slope in Fig. 2b indicates that the generation rate of e_{aq}^- was about $(62.12 \pm 3.73) \mu\text{M min}^{-1}$ per mM phenol here. The degradation rate of MCAA was then almost independent of the phenol concentration (above 0.3 mM) for the quenching of e_{aq}^- by phenol ($2.0 \times 10^7 \text{ M}^{-1} \text{ s}^{-1}$ for $\text{C}_6\text{H}_5\text{OH}$ and $4.0 \times 10^6 \text{ M}^{-1} \text{ s}^{-1}$ for $\text{C}_6\text{H}_5\text{O}^-$) [1]. $\text{C}_6\text{H}_5\text{O}^-$ is the major form of phenol (more than 99% in molar ratio) at pH 12.0 (Fig. S3a), and k showed a similar correlation with the UV absorption by $\text{C}_6\text{H}_5\text{O}^-$ (Text S3 and Fig. S4). Therefore, $\text{C}_6\text{H}_5\text{O}^-$ might be the principal form that induced the generation of e_{aq}^- for the degradation of MCAA in the process. Meanwhile, $\text{C}_6\text{H}_5\text{OH}$ might be the less important form, since its molar ratio is much lower (less than 1%) at pH 12.0 (Fig. S3a), and its absorption at 253.7 nm is much weaker (Fig. S3b). However, its role on the generation of e_{aq}^- in the process might also be essential and shouldn't be ruled out immediately. Fig. 2c shows the correlation between the concentration ratio of MCAA to phenol degraded and the initial phenol concentration in the process. The ratio was around 2.00 and almost independent of the phenol concentration.

3.2.2. Monochloroacetic acid (MCAA)

As an electron-acceptor [1], MCAA has to compete against some other competitors for the e_{aq}^- quenching in the process. Fig. 3a shows the degradation efficiency of MCAA with the MCAA concen-

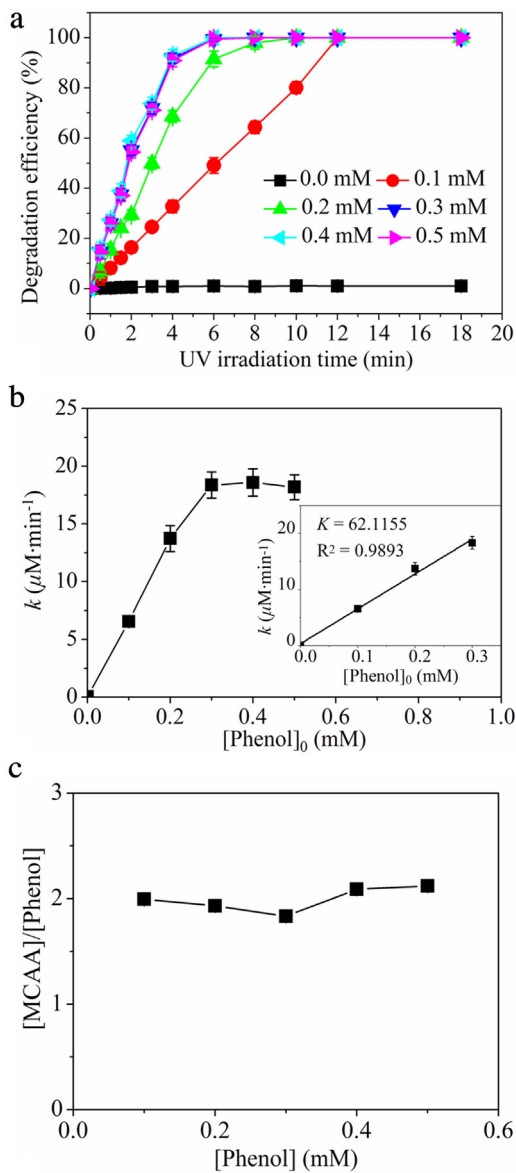


Fig. 2. (a) Influence of phenol concentration (0.0–0.5 mM) on the degradation efficiency of MCAA (80 μM) in the phenol/UV process at pH 12.0. (b) The correlation between the pseudo-zero-order rate constant (k) and the phenol concentration. [Inset: Dependence of the pseudo-zero-order rate constant (k) on the phenol concentration (below 0.3 mM).] The solid line indicates the best linear fit (b). (c) The correlation between the concentration ratio of MCAA to phenol degraded and the initial phenol concentration.

tration ranging from 25 μM to 250 μM in the process at pH 12.0. Actually, since the UV absorption at 253.7 nm is weak [20], MCAA is not competitive with $\text{C}_6\text{H}_5\text{O}^-$ for UV absorption at this wavelength (Fig. S3b) in the process at pH 12.0. MCAA may only have an impact on the involved side reactions of e_{aq}^- , which are parallel competing reactions [25]. Higher initial concentration of MCAA can minimize the side reactions of e_{aq}^- [23] to obtain higher degradation rate constant, which was confirmed by Fig. 3b. The result in Fig. 3b shows the correlation between k and the MCAA concentration. A maximum k was observed when the initial concentration ratio of MCAA to phenol was 1:1. The deceleration in Fig. 3b might be induced by the rapid quenching of e_{aq}^- by some intermediates, which were more efficient than MCAA for the quenching. Fig. 3c shows the correlation between the concentration ratio of MCAA to phenol degraded and the initial MCAA concentration in the process. As can be seen in Fig. 3c, the utilization ratio of phenol for the

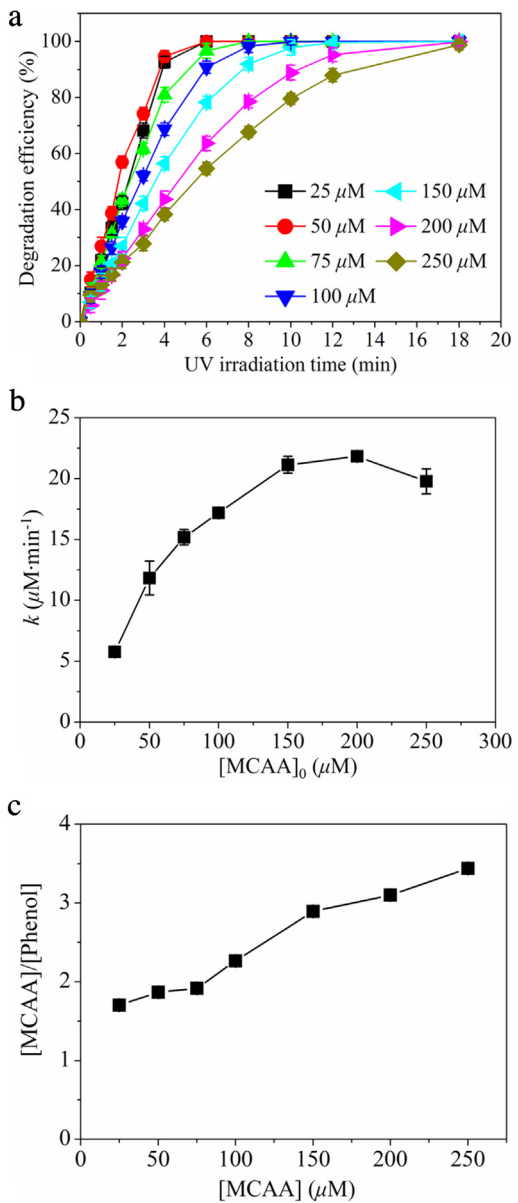


Fig. 3. (a) Influence of MCAA concentration (25–250 μM) on the degradation efficiency of MCAA in the phenol/UV process at pH 12.0. (b) The correlation between k and the MCAA concentration (25–250 μM) at pH 12.0. (c) The correlation between the concentration ratio of MCAA to phenol degraded and the initial MCAA concentration.

generation of e_{aq}^- was promoted with the increase of MCAA, and it is predictable that the limiting ratio was more than 3.00.

3.2.3. pH

The solution pH can govern the molar ratio of $\text{C}_6\text{H}_5\text{O}^-$ (Fig. S3a), which may have a significant influence on the generation of e_{aq}^- for the degradation of MCAA in the process. Thus, the influence of pH on the degradation efficiency of MCAA was investigated with pH from 6.2 to 12.3. As shown in Fig. 4a, it is obvious that the degradation efficiency was pH-dependent with a maximum obtained at pH 12.3. Fig. 4b shows the correlation between k and pH, and the curve almost coincided with the molar ratio of $\text{C}_6\text{H}_5\text{O}^-$ versus pH (Fig. S3a) except for the degradation at pH below 8.4. The molar ratio of $\text{C}_6\text{H}_5\text{O}^-$ at pH below 8.4 is negligible (less than 3%), while, the degradation of MCAA (by e_{aq}^- , Fig. 1b and Table 1) was considerable, and the existence of $\text{C}_6\text{H}_5\text{OH}$ might account for the

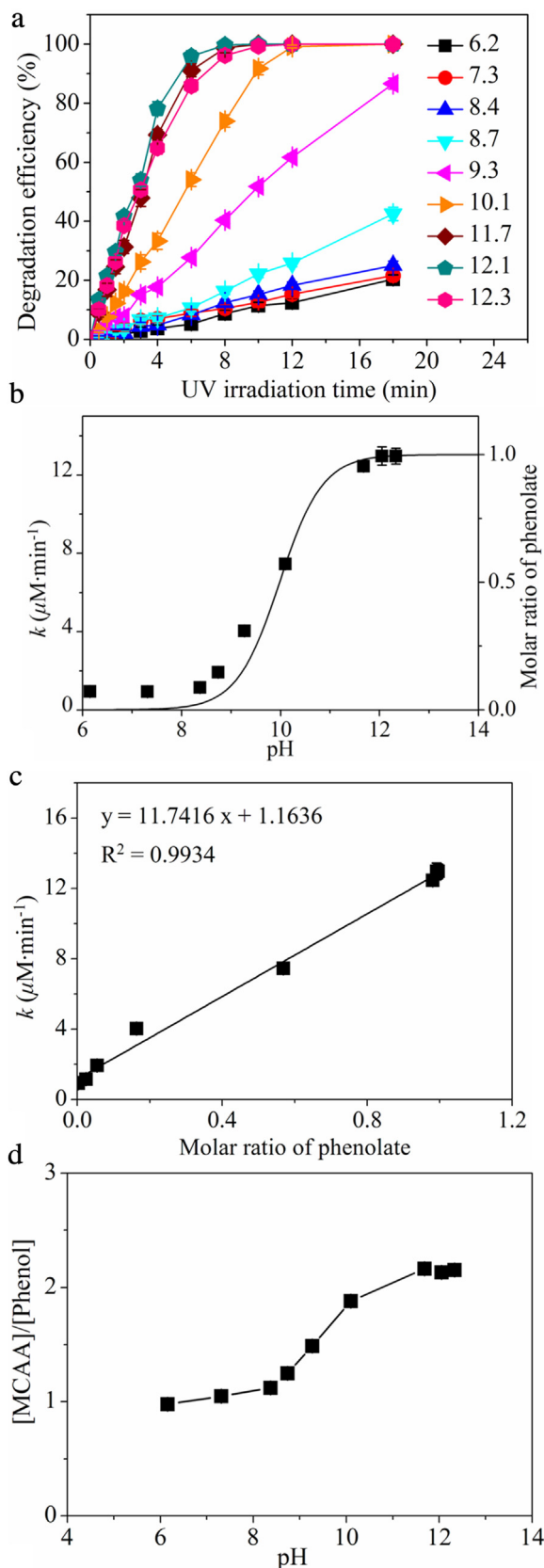
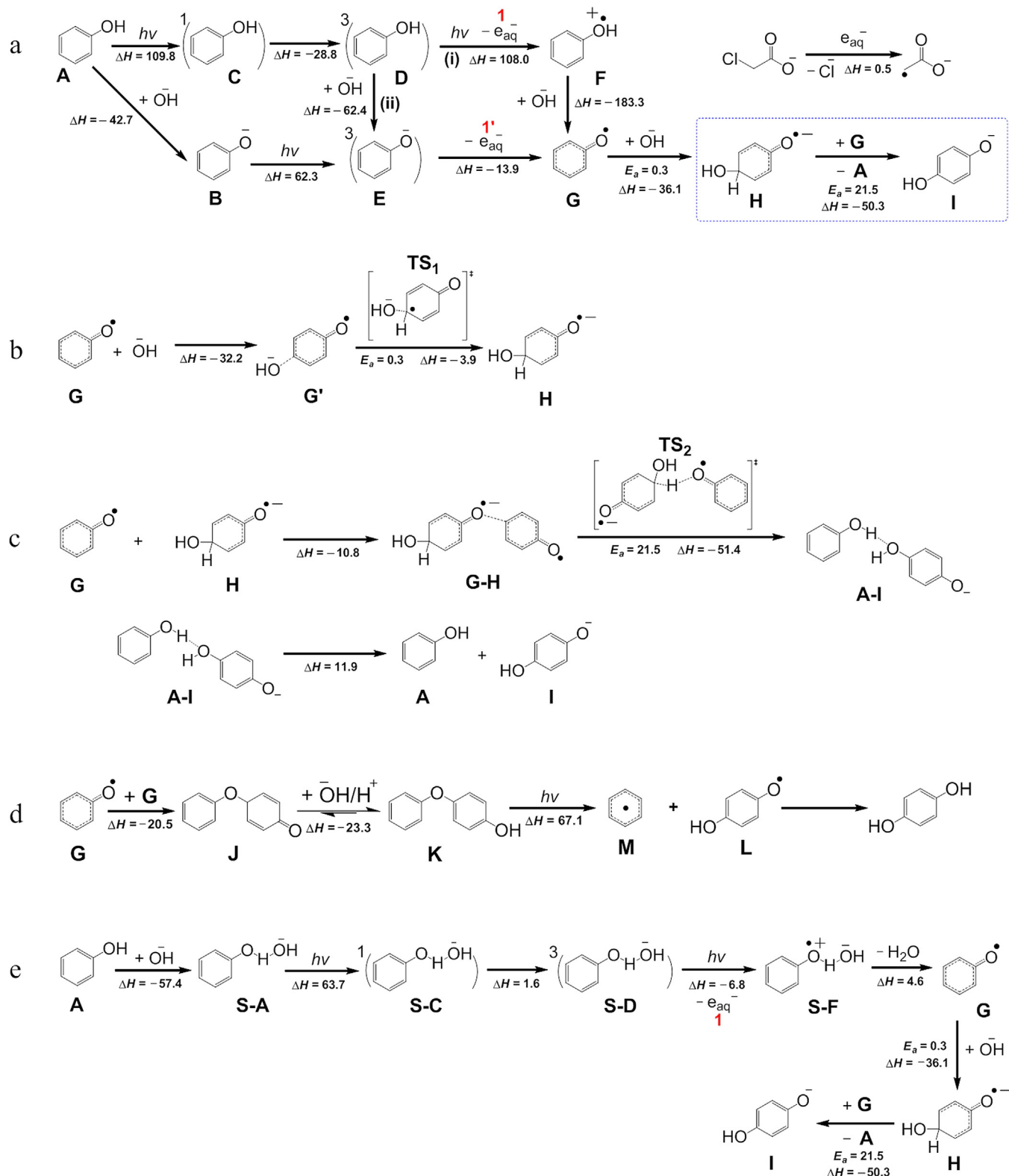


Fig. 4. (a) Influence of pH (6.2–12.3) on the degradation efficiency of MCAA ($80 \mu\text{M}$) in the phenol/UV process. (b) The pseudo-zero-order rate constant (k) versus pH (6.2–12.3). The solid line part b is the pH dependent distribution of $\text{C}_6\text{H}_5\text{O}^-$ (Fig. S3a). (c) The pseudo-zero-order rate constant (k) versus the molar ratio of $\text{C}_6\text{H}_5\text{O}^-$. The solid line indicates the best linear fit (c). (d) The correlation between the concentration ratio of MCAA to phenol degraded and pH.

exception. Generally, it is assumed that photolysis of $\text{C}_6\text{H}_5\text{OH}$ does not produce e_{aq}^- or with negligible quantum yields [26]. However, e_{aq}^- ejection from $\text{C}_6\text{H}_5\text{OH}$ by flash photolysis has been examined [16,27]. It has been postulated that (i) the ejection of proton from excited $\text{C}_6\text{H}_5\text{OH}$ leads to excited $\text{C}_6\text{H}_5\text{O}^-$, which can release electron [27], and the newly generated electron is then quenched by proton to H^\bullet rapidly ($2.3 \times 10^{10} \text{ M}^{-1} \text{ s}^{-1}$) [1]; (ii) excited $\text{C}_6\text{H}_5\text{OH}$ ejects an electron to form $\text{C}_6\text{H}_5\text{OH}^\bullet$ radical, which can release a proton to capture the newly isolated electron rapidly [16]. According to Fig. 1b and Table 1, e_{aq}^- was indeed generated in the process even at pH 6.2, being the dominant reactive species. Meanwhile, as a proton-coupled electron transfer (PCET) reagent, $\text{C}_6\text{H}_5\text{OH}$ can easily release electron without H^\bullet formation via multiple site electron–proton transfer (MS-EPT) pathway [28], which was validated by Fig. 4c. The result in Fig. 4c shows that k had a positive linear dependence on the molar ratio of $\text{C}_6\text{H}_5\text{O}^-$, which indicates that the generation of e_{aq}^- was induced by photolysis of $\text{C}_6\text{H}_5\text{O}^-$ and $\text{C}_6\text{H}_5\text{OH}$ (Text S4). According to Fig. 4c, the rates of the generation of e_{aq}^- from $\text{C}_6\text{H}_5\text{OH}$ and $\text{C}_6\text{H}_5\text{O}^-$ were $(1.16 \pm 0.20) \mu\text{M min}^{-1}$ and $(12.91 \pm 0.34) \mu\text{M min}^{-1}$ per 0.2 mM phenol, respectively (Text S4). It is obvious that the generation of e_{aq}^- induced by photolysis of $\text{C}_6\text{H}_5\text{O}^-$ was much more efficient (about 10 times) than that by photolysis of $\text{C}_6\text{H}_5\text{OH}$, which was consistent with the dependence of the e_{aq}^- generation upon pH reported by Bussandri et al. [19]. The dependence was corroborated by Fig. 4d. The result in Fig. 4d shows the correlation between the concentration ratio of MCAA to phenol degraded and pH in the process, and the ratio increased from 0.97 to 2.15 with pH ranging from 6.2 to 12.3, meaning that less phenol was required for the degradation of MCAA at higher pH.

3.3. Mechanism of the generation of e_{aq}^- in the phenol/UV process

The identification of stable products from the generation of e_{aq}^- in the process was achieved by GC/MS-MS, as shown in Fig. S5. It indicates that *p*-benzoquinone was the stable product from phenol in the process. Moreover, the identification of *p*-benzoquinone (Fig. S5) could indirectly confirm the formation of *p*-hydroquinone in the process. According to the study reported by Joschek et al., phenol could be transformed to *p*-benzoquinone with *p*-hydroquinone as the intermediate [14]. The formation of *p*-hydroquinone was induced by cleavage reaction of the dimerization product, which was formed from the carbon–oxygen dimerization of $\text{C}_6\text{H}_5\text{O}^\bullet$ [14,17]. The transformation of phenol to *p*-hydroquinone was designated as period I, and the oxidation of *p*-hydroquinone to *p*-benzoquinone was period II. Quantitatively, one mole of phenol could eject one mole of e_{aq}^- and $\text{C}_6\text{H}_5\text{O}^\bullet$ [14], and one mole of *p*-hydroquinone could eject two moles of e_{aq}^- and one mole of *p*-benzoquinone with the disproportionation of *p*-benzoquinone radical [14]. At most, one mole of phenol could eject three moles of e_{aq}^- with *p*-benzoquinone as the product [14], which was inconsistent with the result from Fig. 3c. The result in Fig. 3c indicates that one mole of phenol was potential to degrade more than three moles of MCAA, in other words, more than three moles of e_{aq}^- could be ejected from one mole of phenol with the formation of some stable products (*p*-benzoquinone) under these conditions. Moreover, the dependence of the ratio on pH in Fig. 4d cannot be interpreted by the transformation pathway reported by Joschek et al. [14,17]. Thus, a transformation pathway for the period I was proposed to interpret the inconsistency, and it was displayed in Scheme 1a and supported by the DFT based calculations. The generation of e_{aq}^- from *p*-hydroquinone in period II was not shown in the present work, and it could be seen in the previous research reported by Joschek et al. [14].



Scheme 1. (a) Proposed pathway for the transformation of phenol and MCAA in the phenol/UV process. (b) Proposed pathway for the transformation from phenoxyl radical to the adduct. (c) Proposed pathway for the transformation from the adduct of phenoxy radical and OH⁻ to *p*-hydroquinone anion. (d) Proposed pathway for the formation of *p*-hydroquinone by cleavage reaction of the dimerization product. (e) Proposed pathway involving MS-EPT for the transformation of phenol in the phenol/UV process. The energies (relative enthalpies) reported herein were calculated with zero-point energy (ZPE) correction and given in kcal mol⁻¹.

3.3.1. The recycling of C₆H₅O[•]

The photoionization of phenols in water is biphotonic [29] with the first excited singlet states and the first triplet states as the intermediates [16], and it is distinct from that of their anions, which is

monophotonic [29] with the first triplet states as the intermediates [16]. Moreover, the first triplet states are the precursors of the phenoxyl radicals and e_{aq}⁻ [16,29]. As shown in Scheme 1a, C₆H₅OH (A) and C₆H₅O⁻ (B) could eject one mole of e_{aq}⁻ and

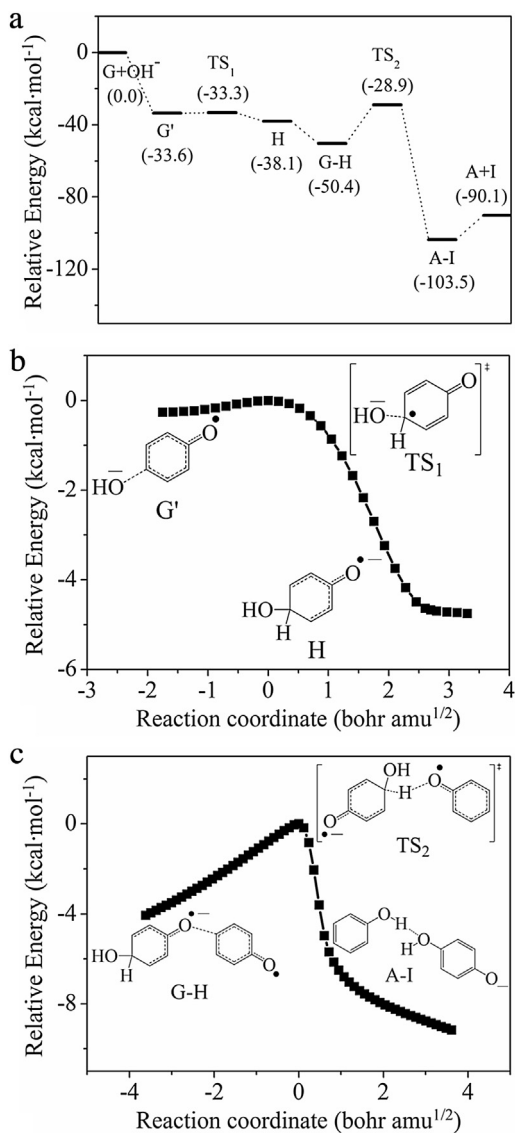


Fig. 5. (a) Energy profiles of minimum energy path (MEP) for the transformation pathway from **G** to **I** involved in **Scheme 1** calculated at the B3LYP/6-311++G (3df, 3pd) level of theory. (b) Calculated MEP of reaction from **G'** to **H**. (c) Calculed MEP of reaction from **G-H** to **A-I**.

$C_6H_5O^\bullet$ (**G**), which are biphotonic [29] and monophotonic [29], respectively. Instead of dimerization (**Scheme 1d**) [14], **G** could generate **H** with the addition of OH^- , which was reported by Joschek et al. [14] and Tomkiewicz et al. [18]. The energy barrier of the reaction $G+OH^- \rightarrow H$ was calculated to be 0.3 kcal mol⁻¹ with **TS₁** as the transition state (Fig. 5a and Scheme 1b), and the intrinsic reaction coordinate (IRC) calculation showed that **TS₁** was connected to **G'** (the adduct of **G** and OH^-) and **H** (Fig. 5b). **H** was then thermodynamically feasible to transform to p -HOC₆H₄O[·] (**I**) with hydrogen abstraction by another **G**, as reported by Tomkiewicz et al. [18], which was exothermic by 50.3 kcal mol⁻¹ with the simultaneous regeneration of **A** from **G**, and the regenerated **A** could eject another e_{aq}^- . The energy barrier of the reaction $G+H \rightarrow A+I$ was calculated to be 21.5 kcal mol⁻¹ with **TS₂** as the transition state (Fig. 5a and Scheme 1c), and the IRC calculation showed that **TS₂** was connected to **G-H** and **A-I** (Fig. 5c). Totally, with the recycling of $C_6H_5O^\bullet$, one mole of phenol could indeed eject two moles of e_{aq}^- with p -hydroquinone as the product in period I. The recycling of $C_6H_5O^\bullet$ was essential for the formation of p -hydroquinone (in period I) and p -benzoquinone (in period II) from phenol. The trans-

formation was different from that reported by Joschek et al. [14,17], and with an energy barrier of 21.5 kcal mol⁻¹, the transformation from $C_6H_5O^\bullet$ to p -hydroquinone in **Scheme 1a** (−86.4 kcal mol⁻¹) was much more feasible and efficient than that in **Scheme 1d** with the endothermic photolysis of 4-phenoxyphenol (**K**) as the rate-determining step (67.1 kcal mol⁻¹). Kinetically, the energy barrier of the electron release from **B** was 62.3 kcal mol⁻¹, which was much lower than that from **A** (109.8 kcal mol⁻¹) by 47.5 kcal mol⁻¹. It is obvious that the generation of e_{aq}^- induced by photolysis of C_6H_5OH , which theoretically verified the dependence of the generation of e_{aq}^- on pH in the process (Fig. 4a and b).

3.3.2. MS-EPT pathway

While, the energies for the excitation of **A** to its first excited singlet state **C** (109.8 kcal mol⁻¹) and the electron ejection from **D** (108.0 kcal mol⁻¹) were so high that UV irradiation at 253.7 nm (112.7 kcal mol⁻¹) cannot accomplish the process efficiently. Fortunately, with OH^- as the proton-acceptor base involved in the process, a MS-EPT pathway helped to lower the energies for the excitation, which was proposed in **Scheme 1e**, and a significant decline of 46.1 kcal mol⁻¹ in the energy for the excitation from 109.8 kcal mol⁻¹ (**A**) to 63.7 kcal mol⁻¹ (**S-A**) was observed. The importance of the MS-EPT pathway is determined by the basicity of the proton-acceptor base [28], and it is reasonable to select OH^- as the proton-acceptor base, since OH^- ($pK_b = -1.7$ [28]) is much more basic than HPO_4^{2-} ($pK_b = 6.8$ [28]).

The involvement of proton-acceptor base (OH^-) in the process induced the simultaneous transfer of electron and proton to avoid the formation of high-energy intermediate via MS-EPT pathway [28], which facilitated the generation of e_{aq}^- from C_6H_5OH thermodynamically. As shown in **Scheme 1e**, the initial adducts $C_6H_5OH \cdots OH^-$ (**S-A**) formation occurred with H-bond interaction [28,30], which could shorten the distance between the proton donor (C_6H_5OH) and the proton acceptor (OH^-) (Fig. S1) [30]. With the first photon absorbed, **S-A** was excited to the first excited singlet state (**S-C**), and then to the first triplet state (**S-D**) through intersystem crossing, followed by MS-EPT pathway with the second photon absorbed. In the MS-EPT step, electron transfer occurred to MCAA and proton transfer to OH^- , and these two events were spatially separated without H^\bullet formation. Moreover, hydrated phenoxyl radical ($C_6H_5O^\bullet \cdots H_2O$) (**S-F**) was generated instead of protonated phenoxyl radical ($C_6H_5OH^\bullet$) (**F**), which is higher-energy intermediate (Table S1).

As a key factor [28], the involved H-bond interaction in the process did alter the properties of C_6H_5OH and $C_6H_5OH^\bullet$, as shown in Fig. S1. With the release of e_{aq}^- from **S-A**, the bond length of the hydrogen-oxygen of the hydroxyl was changed from 1.643 Å (**S-A**) to 1.900 Å (**S-F**) (Fig. S1), and it could be thought that electron-proton transfer from **S-A** to different acceptors (MCAA and OH^-) occurred simultaneously without formation of H^\bullet , which was the MS-EPT pathway [28] (Text S1.2). The stabilization of C_6H_5OH and $C_6H_5OH^\bullet$ by OH^- with H-bond interaction (**Scheme 1e**) made the properties of C_6H_5OH and $C_6H_5OH^\bullet$ similar to those of $C_6H_5O^-$ and $C_6H_5O^\bullet$, respectively (Text S1.2 and Fig. S1). The stabilization by OH^- also made the e_{aq}^- release from C_6H_5OH much more efficient without formation of higher-energy intermediate ($C_6H_5OH^\bullet$) (**Scheme 1**). The energy barrier (63.7 kcal mol⁻¹) was moderate and similar to its conjugate base, namely $C_6H_5O^-$ (62.3 kcal mol⁻¹).

3.3.3. Theoretical verification of experiment

According to Fig. 2c, the ratio was around 2.00, and it was reasonable that the generation of e_{aq}^- from phenol ($C_6H_5O^-$ here) was via the pathway of period I in **Scheme 1a** with numerous phenol in the solution. The positive linear correlation in Fig. 2b and S4 also confirmed the generation of e_{aq}^- from $C_6H_5O^-$ in period I with-

out that from *p*-hydroquinone in period II. It was obvious that the transformation of $C_6H_5O^\bullet$ to p -HOC $_6H_4O^-$ (from **G** to **I** in **Scheme 1a** and 1e) was dependent on the OH $^-$ concentration, namely pH. The regenerated C_6H_5OH was responsible for the generation of the second e_{aq}^- (period I), which was also pH-dependent (Fig. 4a and 4b). It was acceptable that the ratio in Fig. 4d increased from 0.97 to 2.15 with pH from 6.2 to 12.3, which confirmed the dependence of the generation of the second e_{aq}^- on pH. The generation of e_{aq}^- from phenol in period I was confirmed by the maximum ratio at pH 12.3. Thus, it was predictable that the generation rate of e_{aq}^- from $C_6H_5O^-$ in Fig. 2b [(62.12 ± 3.73) $\mu M min^{-1}$ per mM phenol)] was consistent with that in Fig. 4c [(12.91 ± 0.34) $\mu M min^{-1}$ per 0.2 mM phenol], since the generation rates in Fig. 2b and 4c were both from $C_6H_5O^-$ in period I. Theoretically, one mole of phenol could eject four moles of e_{aq}^- via period I (**Scheme 1a** and 1e) and period II, which could interpret the limiting ratio in Fig. 3c. The increase of MCAA concentration could promote the quenching of e_{aq}^- ejected from $C_6H_5O^-$ via period I (**Scheme 1a** and 1e), which would induce the simultaneous accumulation of *p*-hydroquinone. The accumulation could induce the generation of e_{aq}^- via period II, and the ratio was then more than 2.00 and approaching 4.00. Meanwhile, *p*-benzoquinone could be generated (Fig. S5) and accumulated to quench e_{aq}^- ($1.25 \times 10^9 M^{-1} s^{-1}$) [31], which might account for the deceleration in Fig. 3b. According to **Scheme 1a** and 1e, the energy barriers of the electron release from **B** and **S-A** were 62.3 kcal mol $^{-1}$ and 63.7 kcal mol $^{-1}$ respectively, and the difference of the energy barriers validated that higher pH promoted the generation of e_{aq}^- from phenol in period I, as shown in Fig. 4a and 4b. Eventually, the moderate energy barriers and the consistency of the experimental and theoretical results corroborated the rationality of the proposed transformation mechanism. The essential recycling of $C_6H_5O^\bullet$ for the generation of the second e_{aq}^- and the formation of *p*-hydroquinone was theoretically confirmed and experimentally demonstrated. The recycling was crucial for the generation of e_{aq}^- from phenol with a limiting ratio of 4.00.

3.4. Quantum yield of e_{aq}^- in the phenol/UV process

$C_6H_5O^-$ can quench e_{aq}^- to induce the side reaction of e_{aq}^- at pH 12.0 [1], but it is acceptable to apply the degradation kinetics of MCAA to express the quantum yield of e_{aq}^- in the phenol/UV process, since the quenching of e_{aq}^- by $C_6H_5O^-$ is inefficient ($4.0 \times 10^6 M^{-1} s^{-1}$) [1]. The quantum yield (Φ , mol/einstein) [32] of e_{aq}^- in the phenol/UV process is defined as the ratio of the moles of the generated e_{aq}^- (**Scheme 1a** and 1e) to the moles of the photons absorbed by $C_6H_5O^-$. $\Phi = (0.250 \pm 0.015) mol/einstein$ was calculated with the method described in a previous work [4], assuming that e_{aq}^- generated for the dechlorination of MCAA did not have any side reactions under these conditions. $\varepsilon(C_6H_5O^-) = 942.43 M^{-1} cm^{-1}$ at 253.7 nm (Text S2 and Fig. S3b) and the slopes of the positive linear correlation obtained in Fig. 2b were applied for the calculation. The positive linear correlation in Fig. 2b indicates that the generation rate of e_{aq}^- was about (62.12 ± 3.73) $\mu M min^{-1}$ per mM phenol at pH 12.0 in the phenol/UV process. The rate was obtained by the generation of e_{aq}^- from $C_6H_5O^-$ in period I, in which $C_6H_5O^\bullet$ and e_{aq}^- was ejected with a ratio of 1:1. Surprisingly, the quantum yield of e_{aq}^- in the phenol/UV process in this present work was consistent with that ($\Phi = 0.23$ [26]) obtained with N₂O as the e_{aq}^- probe.

4. Conclusions

This present work has experimentally and theoretically demonstrated the combination of phenol and UV irradiation (253.7 nm) for the e_{aq}^- generation. A pathway for the transformation of phe-

nol was proposed and confirmed by the DFT based calculations. The intermediate – *p*-hydroquinone was much more readily to be generated from the hydrogen abstraction of the adduct by $C_6H_5O^\bullet$ (rather than from the photolysis of the $C_6H_5O^\bullet$ dimers), which makes it possible to generate four moles of e_{aq}^- from one mole of phenol with *p*-benzoquinone as the product. Furthermore, the decisive role of phenol on the generation of e_{aq}^- in the process was experimentally and theoretically confirmed. The solution pH also played an important role on the generation of e_{aq}^- in the process. Surprisingly, the generation of e_{aq}^- from phenol was considerable at moderate pH (Fig. 4a and b). As phenol derivatives, (+)-catechin, thymol and *p*-cresol showed the similar efficiency for the degradation of MCAA (Fig. S6), which indicates the generation of e_{aq}^- from the phenol derivatives. Moreover, (+)-catechin is abundant in green tea [33] and environmentally friendly [34].

The findings of the phenol/UV process may therefore help to elucidate the mechanism of e_{aq}^- generation from the natural phenolic compounds, which make it possible to find the environmentally benign phenolic compounds (e.g., plant phenolics [13]) to establish novel e_{aq}^- based ARPs for the pollution remediation. More detailed studies for the e_{aq}^- generation mechanism and the relationship between the e_{aq}^- generation efficiency and the structures of phenol derivatives deserve to be focused on.

Acknowledgements

This work was financially supported by the National Natural Science Foundation of China (Grant No. 51178134, 51378141 and 21203042), the Fundamental Research Funds for the Central Universities (Grant No. HIT. NSRF. 2013057), Heilongjiang Provincial Department of Science and Technology (Grant No. PS13H05), and the Open Project of State Key Laboratory of Supramolecular Structure and Materials (JLU) (SKLSSM201620).

Appendix A. Supplementary data

Supplementary data associated with this article can be found, in the online version, at <http://dx.doi.org/10.1016/j.apcatb.2016.07.034>.

References

- [1] G.V. Buxton, C.L. Greenstock, W.P. Helman, A.B. Ross, *J. Phys. Chem. Ref. Data* 17 (2) (1988) 513–886.
- [2] A. Kumar, J.A. Walker, D.M. Bartels, M.D. Sevilla, *J. Phys. Chem. A* 119 (34) (2015) 9148–9159.
- [3] B.P. Vellanki, B. Batchelor, A. Abdel-Wahab, *Environ. Eng. Sci.* 30 (5) (2013) 264–271.
- [4] X. Li, J. Ma, G. Liu, J. Fang, S. Yue, Y. Guan, L. Chen, X. Liu, *Environ. Sci. Technol.* 46 (13) (2012) 7342–7349.
- [5] Y. Qu, C.-J. Zhang, P. Chen, Q. Zhou, W.-X. Zhang, *Chemosphere* 107 (2014) 218–223.
- [6] P. Calza, E. Pelizzetti, *J. Photochem. Photobiol. A: Chem.* 162 (2–3) (2004) 609–613.
- [7] X. Liu, S. Yoon, B. Batchelor, A. Abdel-Wahab, *Sci. Total Environ.* 454–455 (2013) 578–583.
- [8] Z. Song, H. Tang, N. Wang, L. Zhu, *J. Hazard. Mater.* 262 (2013) 332–338.
- [9] B.P. Vellanki, B. Batchelor, *J. Hazard. Mater.* 262 (2013) 348–356.
- [10] L.I. Grossweiner, G.W. Swenson, E.F. Zwicker, *Science* 141 (3583) (1963) 805–806.
- [11] H.-I. Joschek, L.I. Grossweiner, *J. Am. Chem. Soc.* 88 (14) (1966) 3261–3268.
- [12] Y. Zhang, K.A. Simon, A.A. Andrew, R.D. Vecchio, N.V. Blough, *Environ. Sci. Technol.* 48 (21) (2014) 12679–12688.
- [13] V. Cheynier, G. Comte, K.M. Davies, V. Lattanzio, S. Martens, *Plant Physiol. Biochem.* 72 (2013) 1–20.
- [14] H.-I. Joschek, S.I. Miller, *J. Am. Chem. Soc.* 88 (14) (1966) 3273–3281.
- [15] J.C. Mialocq, J. Sutton, P. Goujon, *J. Chem. Phys.* 72 (12) (1980) 6338–6345.
- [16] T. Alapi, A. Dombi, *J. Photochem. Photobiol. A: Chem.* 188 (2–3) (2007) 409–418.
- [17] H.-I. Joschek, S.I. Miller, *J. Am. Chem. Soc.* 88 (14) (1966) 3269–3272.
- [18] M. Tomkiewicz, A. Goren, M. Cocivera, *J. Am. Chem. Soc.* 93 (25) (1971) 7102–7103.
- [19] A. Bussandri, H. van Willigen, *J. Phys. Chem. A* 106 (8) (2002) 1524–1532.

[20] C.H. Jo, A.M. Dietrich, J.M. Tanco, *Water Res.* 45 (8) (2011) 2507–2516.

[21] X. Zhong, S. Royer, H. Zhang, Q. Huang, L. Xiang, S. Valange, J. Barrault, *Sep. Purif. Technol.* 80 (1) (2011) 163–171.

[22] M.D. Liptak, K.C. Gross, P.G. Seybold, S. Feldgus, G.C. Shields, *J. Am. Chem. Soc.* 124 (22) (2002) 6421–6427.

[23] W.M. Draper, D.G. Crosby, *J. Agric. Food Chem.* 31 (4) (1983) 734–737.

[24] P. Wardman, *J. Phys. Chem. Ref. Data* 18 (4) (1989) 1637–1755.

[25] M.-C. Fournier, L. Falk, J. Villermaux, *Chem. Eng. Sci.* 51 (22) (1996) 5053–5064.

[26] J. Jortner, M. Ottolenghi, G. Stein, *J. Am. Chem. Soc.* 85 (18) (1963) 2712–2715.

[27] G. Dobson, L.I. Grossweiner, *Trans. Faraday Soc.* 61 (1965) 708–714.

[28] D.R. Weinberg, C.J. Gagliardi, J.F. Hull, C.F. Murphy, C.A. Kent, B.C. Westlake, A. Paul, D.H. Ess, D.G. McCafferty, T.J. Meyer, *Chem. Rev.* 112 (7) (2012) 4016–4093.

[29] J. Feitelson, E. Hayon, A. Treinin, *J. Am. Chem. Soc.* 95 (4) (1973) 1025–1029.

[30] J. Bonin, C. Costentin, M. Robert, J.-M. Savéant, C. Tard, *Acc. Chem. Res.* 45 (3) (2012) 372–381.

[31] E.J. Hart, S. Gordon, J.K. Thomas, *J. Phys. Chem.* 68 (6) (1964) 1271–1274.

[32] F.J. Beltrán, G. Ovejero, J.F. García-Araya, J. Rivas, *Ind. Eng. Chem. Res.* 34 (5) (1995) 1607–1615.

[33] J.-H. Choi, I.-K. Rhee, K.-Y. Park, K.-Y. Park, J.-K. Kim, S.-J. Rhee, *Life Sci.* 73 (12) (2003) 1479–1489.

[34] S.-J. Kim, J.M. Lee, R.A. Kumer, S.Y. Park, S.C. Kim, I. In, *Chem. Asian J.* 10 (5) (2015) 1192–1197.